Temperature and Magnetic Field-Induced Magnetization Reversal Phenomena in Double Perovskite La2-xBixFeCrO6 (x = 0.1, 0.2, 0.4, and 0.5) polycrystals

Athira P [1] , Krishnamurthy Jyothinagaram [1] , Venimadhav Adyam [2]

1. Physics, National Institute of Technology Andhra Pradesh, Tadepalligudem, IND 2. Cryogenic Engineering Centre, Indian Institute of Technology Kharagpur, Kharagpur, IND

Corresponding author: Athira P, athirapganesh@gmail.com

Abstract

Unlike ferromagnetic materials, uncompensated ferrimagnetic (FiM) systems such as orthovanadates, orthoferrites, and orthochromites exhibit magnetization reversal (MR) and magnetic switching effects without reversing the field direction. The polycrystalline $La_{2-x}Bi_xFeCrO_6$ (x = 0.1, 0.2, 0.4, and 0.5) double perovskite bulk samples are prepared by the conventional solid-state reaction method. The polycrystalline samples were found to be stable in the orthorhombic crystal structure with a space group of *Pnma*, and the field-emission scanning electron microscope micrographs show the cube-shaped grains of size 2-10 μm. The zero-magnetization phenomenon that occurs at compensation temperature well below T_N varies with Bi doping. The formation of Fe and Cr individual magnetic clusters within the FiM matrix behaves independently with temperature in Bi-doped samples and causes the MR effect. The compensation temperature corresponds to zero-magnetization and MR effect is sensitive to the applied Zeeman fields and Bi concentration in disordered $La_{2-x}Bi_xFeCrO_6$ samples. For x = 0.5, the absence of MRE could be attributed to the antiferromagnetic correlations of Fe and Cr spins and the presence of nonmagnetic impurities. The studied materials are promising candidates for the design of thermomagnetic switches, constant-temperature, bath-based magnetic cooling/heating, and magnetic memory elements due to their observed property of pole-reversal phenomena.

Introduction

In oxides and intermetallic compounds, magnetization reversal has drawn a lot of attention lately. Usually, it is achieved by applying a magnetic field in the opposite direction of the aligned spin moments [1]. Without altering the direction of the applied magnetic field, ferrimagnetic (FiM) materials made up of two or more types of antiferromagnetically ordered magnetic ions can show the magnetization reversal effect (MRE), which is the flipping of positive magnetization to negative magnetization or vice versa [2, 3]. Neel made the initial observation of it in systems exhibiting distinct temperature-dependent magnetic behavior [4]. The magnetization fluctuates so that it becomes negative with changing temperatures and is also zero at a point, known as the compensation temperature (T_{comp}). The structure and magnetic properties of mixed metal oxides are incredibly complex, especially when they consist of multiple magnetic phases. These materials are promising candidates for the design of thermomagnetic switches and magnetic memory elements due to the rarity of the pole-reversal phenomenon [5]. Numerous materials, including garnets[6], orthoferrites [7], orthovanadates [8], orthochromites [9, 10], molecular magnets [11, 12], and rare earth-based perovskites [13], have been shown to exhibit MRE. This effect is system-dependent; it may be a result of a single-ion magnetocrystalline anisotropy competition, a first-order structural transition linked to an unquenched orbital angular moment [14], or the opposite alignment of Cr ions with rare-earth ions in chromates at low temperatures [15]. The direction of the magnetic moment in an antiferromagnetic (AFM) material with two distinct sublattices will stay constant with the crystallographic axes in the presence of magnetocrystalline anisotropy. The magnetic moment vectors will vary with temperature and may even equal zero when both sublattices have compensated for each other. Additionally, in certain circumstances, the dominance of the magnetic moment, which is antiparallel to the magnetic field, will result in a negative total magnetization. In a predetermined and practical way, the magnetization reversal effect combined with magnetoelectronics can leverage the enormous technological potential for device applications such as thermomagnetic switches, thermally assisted magnetic random-access memories, and other multifunctional devices. This pole-reversal phenomenon could potentially allow for more efficient or novel ways to control magnetic states in devices. Unfortunately, the low-temperature operation of these compounds is the primary obstacle to their prospective uses. Investigating materials that show magnetization reversal at ambient temperatures is, therefore, essential.

MRE was reported in many rare-earth orthochromites, $RCrO_3$ (R = rare-earth element) [16, 17]. Here, the R^{3+}- Cr^{3+} interaction results in MRE, or negative magnetization. This interaction is directed toward R^{3+} moment, which is opposite to the field direction as well as the Cr^{3+} moment. While lowering the temperature below T_N, the R^{3+} sublattice magnetization increases and the net magnetization becomes negative. This phenomenon is not common in most of the magnetic materials, as it is energetically unstable. However, materials with MRE are potential candidates for magnetization switching without flipping the applied field [10, 11]. Therefore, research on this phenomenon has been focused on many materials to explore the MRE at the ambient temperature, including $RFeO_3$ [18].

In view of the intriguing magnetic and electrical behavior, the double perovskite (DP) materials with the formula $R_2BB'O_6$, where B and B' are transition metals, have drawn much attention from the research community due to their large magnetocaloric effect and magnetoresistance effect below their magnetic ordering [19]. The magnetic characteristics of $R_2BB'O_6$ were significantly affected by the difference in B and B' ions, as well as its crystal structure. Typically, in $3d$-$3d$ couplings, the B-O-B and B'-O-B' are coupled antiferromagnetically, whereas the B-O-B' are coupled ferromagnetically. The coexistence of AFM and ferromagnetic (FM) interactions would result in competing magnetic interactions, and it is the major cause of the fascinating magnetic features of DP systems [20] and has found potential applications in information storage, thermomagnetic switches, constant-temperature, bath-based magnetic cooling/heating, spintronics, and resistive memory devices [21]. The discovery of a huge spontaneous exchange bias effect in multifunctional DP systems such as $La_{1.5}Sr_{0.5}CoMnO_6$ [22], and $Sm_{1.5}Ca_{0.5}CoMnO_6$ [23] has sparked more interest, which would greatly support spin reversal devices. Over the past 20 years, Fe-based DP materials have received significant attention owing to their unique physics, including temperature-induced magnetization reversal, exchange bias, and spin reorientation (SR). The antisite disorder (ASD) is inevitable in DPs as the charge difference between the B and B' sites is small and has significantly impacted their physical properties [24].

A reversal of magnetization caused by the temperature has been reported in certain perovskites. At lower temperatures, $LaFe_{0.5}Cr_{0.5}O_3$ (LFCO) exhibits a negative field-cooled (FC) magnetization [25]. Its magnetic characteristics, however, remain mostly uncertain. LFCO has a perovskite structure with AFM ordering, where Fe and Cr are randomly distributed at the B site, and a Neel temperature of 265 K. According to Vijaya Nandhini et al., the Bi-doped LFCO has an unusual zero magnetization. The compound's Fe- and Cr- clusters are being disrupted by the Bi doping, which were identified as the cause of the negative and zero magnetization [26]. As a result, negative magnetization can be tuned by varying the Bi content. The consequences of negative magnetization, such as magnetization reversal switching and magnetocaloric effect are studied in $La_{1.9}Bi_{0.1}FeCrO_6$ compound [27]. In this report, we studied the negative magnetization effect and magnetization reversal in $La_{2-x}Bi_xFeCrO_6$ (LBFCO) series of compounds with x = 0.1, 0.2, 0.4, and 0.5 and compared them with the parent compound.

Materials And Methods

Polycrystalline LBFCO (x = 0.1, 0.2, 0.4, 0.5) samples were synthesized using the conventional solid-state reaction method. High-purity precursor compounds, like La_2O_3, Bi_2O_3, Fe_3O_4, and Cr_2O_3, were weighed in accordance with stoichiometric ratios, combined, and ground for 2 hours, and then heated for 10 hours at 800 °C. Following that, the powder was made into pellets and sintered at 1000 °C for 24 hours while being ground at intermediate intervals. The final sintering took place at 1050 °C for 24 hours. Using Cu-Kα radiation and a Phillips powder high-resolution X-ray diffractometer, the crystal structural analysis of LBFCO was performed. Using a JEOL-JSM5800 field-emission scanning electron microscope (FESEM), the surface morphology was examined. Temperature and magnetic field-dependent DC magnetization studies were carried out using an Evercool Quantum Design superconducting quantum interference device-vibrating sample magnetometer magnetometer.

Results

Crystal structure

The room-temperature powder X-ray diffraction data the of as-prepared Bi-doped LFCO samples are shown in Figure *1* and were found to be stable in an orthorhombic crystal structure with the *Pnma* space group. The diffraction patterns of the compound exhibit well-defined peaks as shown in Figure *2*, and the refined parameters are close to the parent compound $LaFe_{0.5}Cr_{0.5}O_3$ [25] and Bi-doped $La_{1-x/2}Bi_{x/2}Fe_{0.5}Cr_{0.5}O_3$ [26]. It is observed that there is a presence of secondary phase, La_2O_3 in x = 0.5 compound, at 2θ = 32.6°. It can be seen from Figure *1* that the characteristic diffraction peak with diffraction angle of 56°-60° shifts to a higher angle upon Bi doping for x = 0 to x = 0.2 and then shifts to lower angles for x = 0.4 and 0.5. Rietveld refinement of X-ray diffractometer (XRD) patterns of LBFCO (x = 0, 0.1, 0.2, 0.3, 0.4, 0.5) compounds was conducted using FULLPROF software for the 2θ range from 10° to 90° [28], and the results are presented in Figure *2*. The refined parameters and Wyckoff positions are listed in Table *1*. The crystal structure of the x = 0.1 compound is shown in the inset of Figure *2*(a), visualized using VESTA

software [29]. There is a gradual decrease in the lattice parameters of a, b and volume with the increase in dopant concentration.
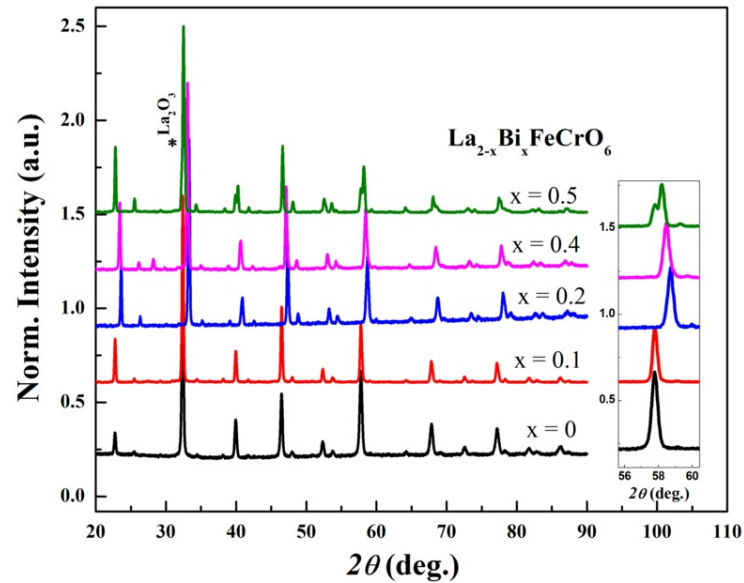

FIGURE 1: Comparison of XRD data of LBFCO samples for x = 0, 0.1, 0.2, 0.4, and 0.5 and the magnified diffraction peaks at 56°-60°
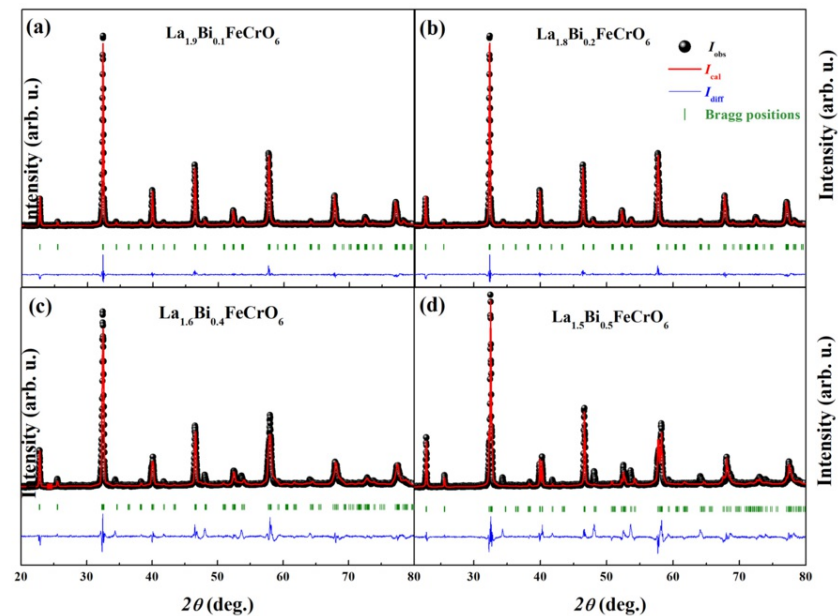
XRD, X-ray diffractometer; LBFCO, $La_{2-x}Bi_xFeCrO_6$

FIGURE 2: Refined XRD patterns of LBFCO compound for (a) x = 0.1, (b) x = 0.2, (c) x = 0.4, and (d) x = 0.5 and the crystal structure of x = 0.1 compound is shown in the inset of Figure 2(a)

XRD, X-ray diffractometer; LBFCO, $La_{2-x}Bi_xFeCrO_6$

The FESEM micrographs of LBFCO (x = 0.1, 0.2, and 0.5) samples are shown in Figure 3. This shows the homogeneous distribution of cubic-shaped grains for x = 0.1 and x = 0.2 with particle sizes of 2-10 μm. In the case of x = 0.5 doping (Figure 3(c)), the particles have more platelet-like structure and are more closely packed than the x = 0.1 and 0.2 doped samples, so the voids are reduced. The particle size of the sample gradually increases with the Bi content.

x		0.1	0.2	0.4	0.5
Lattice parameters					
a (Å)		5.5278	5.5248	5.4941	5.4815
b (Å)		7.8166	7.8125	7.7860	7.7825
c (Å)		5.5395	5.5364	5.5330	5.5424
V (Å^3)		239.3567	238.9666	236.6852	236.4372
Wyckoff positions					
La/Bi in 4c	x	0.0247	0.0251	0.0186	0.0247
	y	0.2500	0.2500	0.2500	0.2500
	z	0.9961	0.9963	1.0118	0.9961
Fe/Cr in 4b	x	0	0	0	0
	y	0	0	0	0
	z	0.5000	0.5000	0.5000	0.5000
O1 in 4c	x	0.4919	0.4924	0.4578	0.4919
	y	0.2500	0.2500	0.2500	0.2500
	z	0.0708	0.0714	0.0687	0.0708
O2 in 8d	x	0.2907	0.2902	0.2045	0.2907
	y	0.0138	0.0148	0.0151	0.0138
	z	0.7130	0.7133	0.7869	0.7130

TABLE 1: Refined lattice parameters and Wyckoff positions of the prepared La2-xBixFeCrO6 with x = 0.1, 0.2, 0.4, 0.5
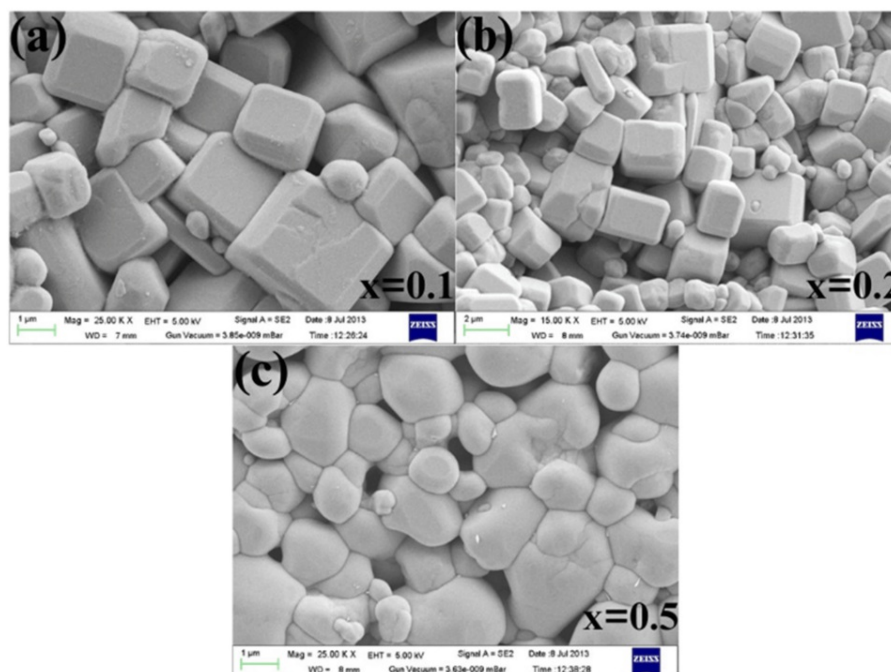
FIGURE 3: FESEM monographs of LBFCO for (a) x = 0.1, (b) x = 0.2, and (c) x = 0.5 doped samples

FESEM, field-emission scanning electron microscope; LBFCO, $La_{2-x}Bi_xFeCrO_6$

Temperature-dependent magnetization study

Figure *4* shows the temperature variation of magnetization (i.e., $M(T)$) study under 100 Oe magnetic field in the zero-field cooled (ZFC), field-cooled cooling (FCC), and field-cooled warming (FCW) modes for LBFCO (x = 0.1, 0.2, 0.4, and 0.5) samples. The measurements are done from 400 K to 3 K, but the magnetic transition, i.e., paramagnetic to FiM or weak ferromagnetic (WFM) transition, is observed above 400 K in the parent compound [26], which is beyond the measured temperature range. Several magnetic characteristics can be observed by lowering the temperature. For all three modes (ZFC, FCC, and FCW), the samples exhibit finite magnetization, which is independent of temperature from 400 K down to 300 K. For x = 0.1 (Figure *4*(a)), $M(T)$ increases and exhibits a bifurcation below 300 K, i.e., irreversibility between FCC and ZFC magnetization below (T_{SR}) ~265 K, where T_{SR} is the spin-reorientation temperature. Due to the reorientation of Fe and Cr magnetic clusters, M_{FCW} and M_{FCC} further drop with temperature and vanish at the compensation temperature (T_{comp}) ~186 K. The negative magnetization below the compensation temperature is due to the magnetocrystalline anisotropy [5]. M_{ZFC} also decreases below T_{SR} and is negative below 135 K. Since there is no thermal hysteresis observed between M_{FCC} and M_{FCW} curves around T_{SR}, the magnetic transition is like a second-order transition.

The observed T_{SR1} value for x = 0.2 is ~246 K, as shown in Figure *4*(b), and there exists a trifurcation between M_{ZFC}, M_{FCC}, and M_{FCW}. M_{FCC} starts decreasing below T_{SR1} and becomes zero at T_{comp1} ~168 K and reaches a maximum value of magnetization 0.57 × 10^{-2} emu/g in the negative direction at 20 K (T_{SR2}), and again increases with another zero magnetization at T_{comp2} ~9.89 K and goes up rapidly until 3 K. M_{FCW} goes undeviated as temperature decreases until 60 K and then increases rapidly until 3 K which matches with the M_{FCC} curve. M_{FCW} is always positive for the entire temperature range. M_{ZFC} starts to increase below T_{SR1} and joins FCC and FCW curves below 6 K. Further, thermal hysteresis between FCC and FCW curves appears in x = 0.2 compound, which could be assigned to the spin-reorientation as observed in $RCrO_3$ (R = rare-earth ion) systems [13]. In the case of x = 0.4 compound, there is a trifurcation below T_{SR1} ~223 K among the M_{ZFC}, M_{FCC}, and M_{FCW} data, and M_{FCC} starts decreasing and becomes negative below T_{comp1} ~195 K. It reaches a maximum value of –0.16 × 10^2 emu/g in the negative direction at 56 K (T_{SR2}) and again starts to increase. Further, it shows zero magnetization again at T_{comp2} ~36 K and increases rapidly until 3 K. M_{FCW} increases slowly until T ~56 K, then increases rapidly with decreasing temperature. M_{ZFC} shows temperature-independent magnetization until 70 K, and there is a

small hump near to 48 K; further, it decreases almost to zero.

On the other hand, it is observed that no negative magnetization appeared for the x = 0.5 compound in the measured temperature regime as shown in Figure 4(d). M_{ZFC} increases slowly and shows an AFM like transition around T_{N1} ~ 245 K, then increases rapidly until 54 K and then decreases. FCC and FCW curves increase with the decreasing temperature, and at T_{N1} ~ 245 K, it bifurcates and M_{FCC} increases slowly until 50 K and then rapidly down to 3 K. M_{FCW} increases and shows a kink at 34 K (T_{N2}) and again increases rapidly. M_{FCW} increases with decreasing temperature and shows a kink at 34 K and again increases and matches the FCC data. This could be an AFM coupling among the sublattices of Fe and Cr without cluster formation. There could be a discrepancy in the magnetization data of x = 0.5 compound due to the impurity present. A neutron diffraction study is required to confirm the actual arrangement of Fe and Cr spin structures.

As shown in the inset of Figure 4(a), the x = 0 compound shows no negative or zero magnetization present, which shows a conventional AFM-like behavior. Kang Yi et al. reported that there is no zero magnetization observed for La_2FeCrO_6 for 500 Oe field [30], but in the case of single perovskite $LaFe_{0.5}Cr_{0.5}O_3$, zero and negative magnetization are observed for a 1000 Oe field due to the ASD present in the octahedral sublattice [25]. A phenomenological model was proposed by Tamine et al. [31] to explain the observation of zero magnetization and the magnetic irreversibility between M_{FCC} and M_{ZFC} just below T_N. In the present systems, a cubic lattice exists in which two uncompensated weak ferromagnets are randomly distributed and antiferromagnetically coupled. Above Neel temperature, the Fe and Cr clusters interact with WFM, while below T_N, the clusters reorient and become antiparallel to one another. The resultant magnetization is zero at the compensation temperature, where these two ordering and magnetization substructures are equal in magnitude but opposite in direction. The overall magnetization of the sample is directed against the direction of the applied field below T_{comp}, and the magnetic moment of the Fe^{3+} clusters, which are aligned antiparallel to the field, can rise faster than that of the Cr^{3+} clusters, which are aligned parallel to the field. The local anisotropy field is responsible for retaining this configuration and a strong external magnetic field is required to change the magnetization completely in the positive direction, with both clusters aligned parallel to the field. It is observed that for x = 0.2 and 0.4, there are two compensation temperatures.
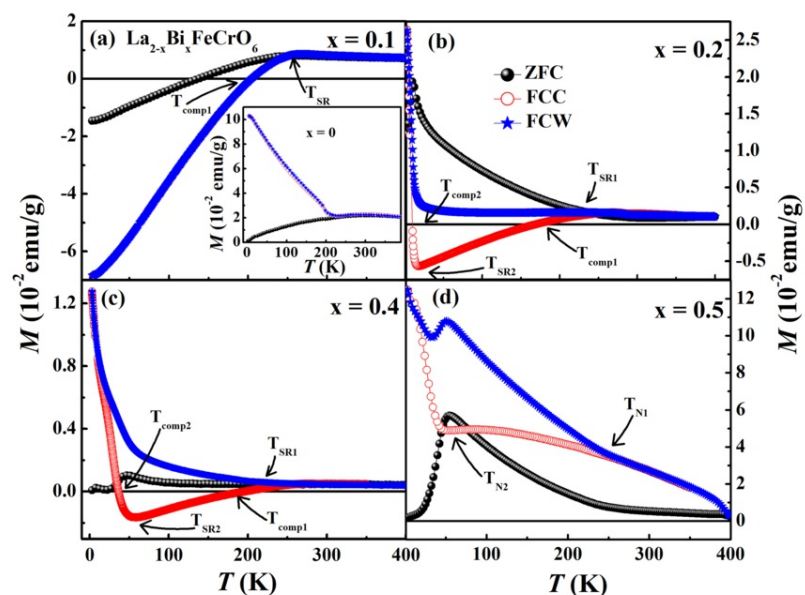

FIGURE 4: Temperature dependence of magnetic susceptibility for La2-xBixFeCrO6 with (a) x = 0.1, (b) x = 0.2, (c) x = 0.4, and (d) x = 0.5 for 100 Oe magnetic field. The inset of figure 4(a) shows the M(T) measurements for x = 0 at 100 Oe

ZFC, zero-field cooled; FCC, field-cooled cooling; FCW, field-cooled warming

There are certain magnetic materials showing similar behavior to $TmCrO_3$ [32], $ErFeO_3$ [33], $GdCrO_3$ [34], and $SmCr_{0.85}Mn_{0.15}O_3$ [35]. Once it crosses the T_{comp1}, it shows a maximum magnetization in the negative direction, and again the Fe clusters start to reorient in the applied field direction. Down to 3 K the total magnetization of the system starts increasing and becomes positive, crossing T_{comp2}. The zero magnetization is observed in the temperature range of 9-205 K. The temperature-dependent magnetic behavior of each sublattice determines its relative contribution to the resulting magnetization [10].
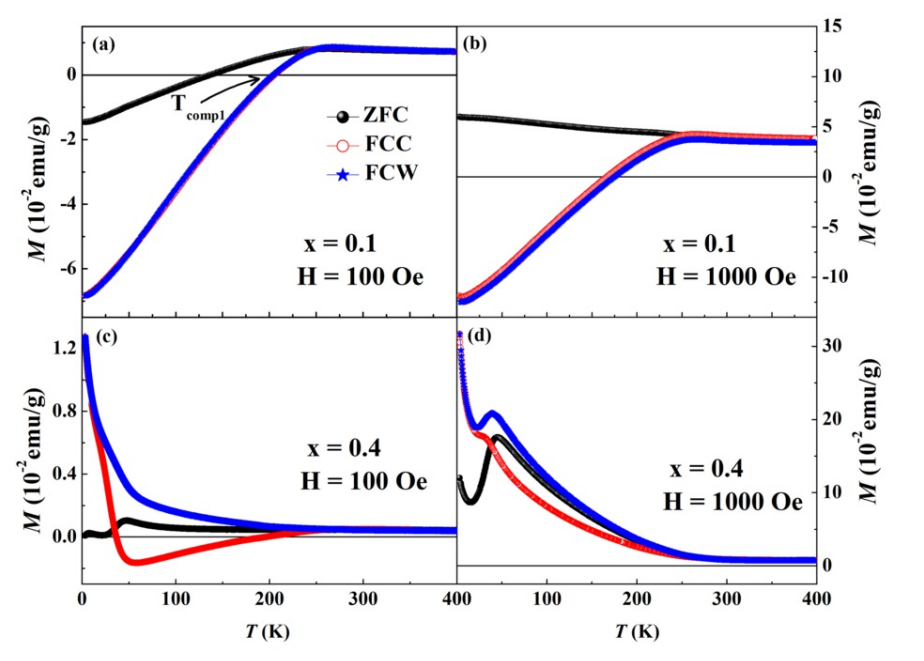
FIGURE 5: M(T) data comparison for x = 0.1 and 0.4 samples at (a) and (c) 100 Oe and (b) and (d) at 1000 Oe magnetic fields, respectively

ZFC, zero-field cooled; FCC, field-cooled cooling; FCW, field-cooled warming

$M(T)$ curves were compared for the x = 0.1 and 0.4 samples at two different magnetic fields, 100 Oe and 1000 Oe as shown in Figure 5. It can be seen that for x = 0.1 sample, at a low magnetic field, all three modes (ZFC, FCC, and FCW) of magnetization show negative values, but for a higher magnetic field, i.e., 1000 Oe, the ZFC curve becomes completely positive, and the compensation temperature for FCC and FCW also shifts to a lower temperature, i.e., ~171 K. In contrast, for the x = 0.4 sample, the negative magnetization and zero magnetization are present only in FCC/FCW modes for a lower magnetic field (100 Oe). With 1000 Oe, all the modes show positive magnetization. Therefore, the negative magnetization also depends on the strength of the applied field. The spin-reorientation temperature (T_{SR}) and compensation temperature (T_{comp}) of all the prepared compounds are shown in Table 2.

x	T_{SR1} (K)	T_{SR2} (K)	T_{comp1} (K)	T_{comp2} (K)	T_N (K)
0.1	265	-	205	-	-
0.2	246	20.4	168	9.8	-
0.4	223	56	182	36	-
0.5	-	-	-	-	34

TABLE 2: Spin reorientation temperature (TSR) and compensation temperature (Tcomp) of La2-xBixFeCrO6 (x = 0.1, 0.2, 0.4, 0.5)

Magnetic field-dependent magnetization study

Figure *6* shows the $M(H)$ hysteresis loop for LBFCO doping samples with sweeping fields of +70 kOe. A clear magnetic hysteresis has been observed for all the samples at low magnetic fields with no tendency toward saturation. As the Bi doping increases, the maximum values of magnetization increase due to the formation of Fe and Cr clusters in the ferrimagnetic lattice. All the compounds show a hysteresis loop at very low magnetic fields and the area of the hysteresis loop increases with Bi content, as shown in the inset of Figure *6*. The values of remnant magnetization (M_r) and coercive field (H_C) show a contrast behavior with Bi doping concentration. The coercive field decrease suggests that the material becomes softer. The increase in M_r may be due to the decrease in oxygen concentration in the sample, as a result, the domain pinning effect has decreased [36].
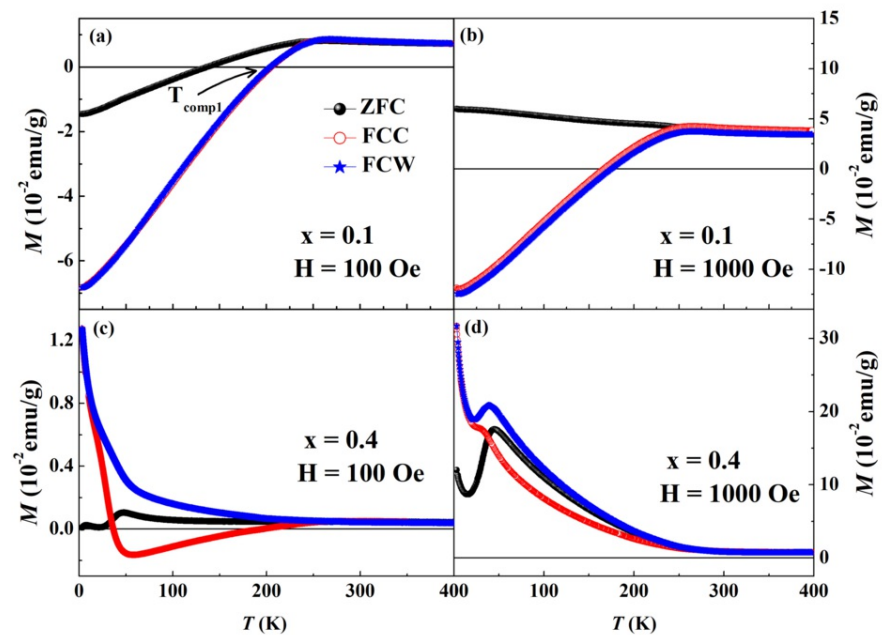
FIGURE 6: M(H) loop of LBFCO (x = 0.1, 0.2, 0.4, and 0.5) samples measured at 5 K, and the inset shows the magnified image of the hysteresis loop.

ZFC, zero-field cooled; FCC, field-cooled cooling; FCW, field-cooled warming

And there is an increase in the slope of the magnetization loop with an increase in the Bi concentration. It is observed that the $x = 0.1$ compound shows the maximum coercive field (H_C) and minimum remnant magnetization (M_r).

Discussion

The most likely explanation for the observed features in Bi-doped LBFCO samples is that there are two kinds of weak ferromagnetic Cr_n and Fe_n domains and clusters that are uncompensated, antiferromagnetically connected, and randomly distributed in the AFM $(Cr_1Fe_1)_n$ matrix, as schematized in Figure *7*, ignoring the impurities present in the higher doped samples ($x = 0.4$ and 0.5). Dipolar interaction causes ferrimagnetic-like behavior because the transverse magnetic components of the Cr_n and Fe_n domains are oriented in opposite directions as a result. One of these two transverse ferromagnetic components will align parallel to the magnetic field, while the other will align antiparallel to it when the magnetic field is applied parallel to it. More clusters are observed in the case of the $x = 0.2$ sample, and the clusters formed decreased for $x = 0.4$ and no clusters are present in the $x = 0.5$ sample, attributing to the absence of MRE. For a critical value of the applied field, the antiparallel component can thus be shifted in the direction of the field by raising the magnetic field. In the same way, temperature has a significant influence on the two tiny ferromagnetic transverse components for Cr and Fe, respectively [20]. There are a number of perovskite systems showing MRE, such as $RCrO_3$ (R = rare-earth ions) [37] Sr_2YbRuO_6 [1], Er_2CoMnO_6 [2], $Ho_2CoMn_{0.6}Ni_{0.4}O_6$ [38], Sm_2CrMnO_6 [39], Gd_2CrMnO_6 [20], $La_{1.5}Sr_{0.5}FeMnO_6$ [19],

Y_2FCrO_6 [21] at temperatures lower than room temperature and the origin of MR effect is different in each system. That is, in Er_2CoMnO_6, it is due to the uniaxial anisotropy of Er^{3+} ions; intrinsic homogeneity is the reason in $La_{1.5}Sr_{0.5}FeMnO_6$, large magnetic moment of rare-earth ion and weak ferromagnetism in $RCrO_3$ results in negative magnetization and so on. The prepared compound, $La_{1.9}Bi_{0.1}FeCrO_6$, shows a spin-reorientation temperature close to room temperature.
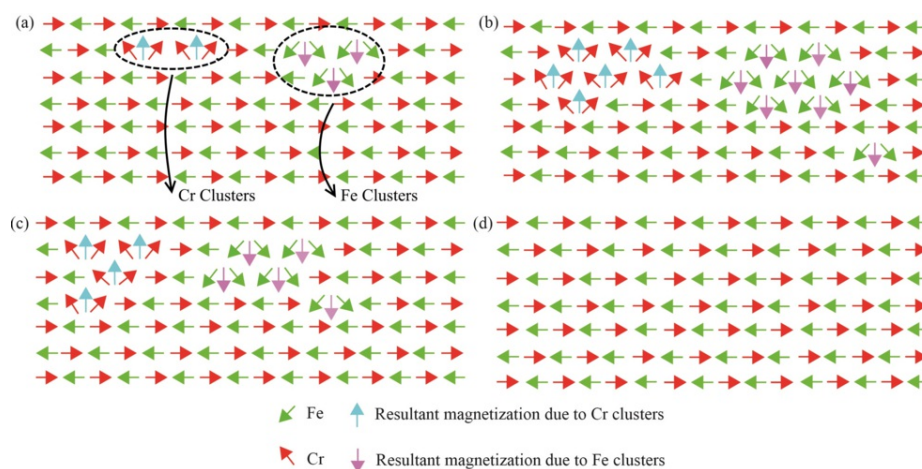
FIGURE 7: Schematized representation of weak ferromagnetic Fen and Crn domains or clusters distributed at random and antiferromagnetically coupled in the La2-xBixFeCrO6 with (a) x = 0.1, (b) x = 0.2, (c) x = 0.4, and (d) x = 0.5 in the ideal condition

Conclusions

In conclusion, we have prepared the polycrystalline $La_{2-x}Bi_xFeCrO_6$ (for x = 0.1, 0.2, 0.4, and 0.5) bulk samples using the conventional solid-state reaction method and studied temperature and magnetic field-dependent magnetization behavior. All the synthesized compounds are formed in an orthorhombic crystal structure with *Pnma* space group. At low magnetic fields and temperatures, the system shows negative magnetization without changing the polarity of the field. This originates from the canting of Fe and Cr clusters at low temperatures, which are antiferromagnetically coupled. The samples with Bi doping content of x = 0.2 and 0.4 show two compensation temperatures with two spin-reorientation transitions, and it has been observed that the T_{SR} decreases with the Bi doping. The MRE depends on the doping concentration and temperature and vanishes for higher applied fields, which is strong enough to overcome magnetocrystalline anisotropy. This is primarily caused by two or more magnetic sublattices with their differing temperature-dependent magnetization behavior from the canting of Fe and Cr clusters coupled antiferromagnetically at low temperatures. Further, in rare-earth magnetic systems, the negative magnetization may occur due to the competition of the rare-earth ion's high magnetic moment and the 3d transition metal ion's weak ferromagnetic behavior. This study would also encourage researchers to develop novel magnetic materials that exhibit magnetization reversal phenomena around the ambient temperature, especially in the Cr-doped M-type hexaferrites. As a result, these materials could be applied in real-world settings such as information storage, thermomagnetic switches, constant-temperature, bath-based magnetic cooling/heating, spintronics, and resistive memory devices.

Additional Information

Author Contributions

All authors have reviewed the final version to be published and agreed to be accountable for all aspects of the work.

Concept and design: Athira P, Krishnamurthy Jyothinagaram, Venimadhav Adyam

Acquisition, analysis, or interpretation of data: Athira P, Krishnamurthy Jyothinagaram, Venimadhav Adyam

Drafting of the manuscript: Athira P, Krishnamurthy Jyothinagaram, Venimadhav Adyam

Critical review of the manuscript for important intellectual content: Athira P, Krishnamurthy

Jyothinagaram, Venimadhav Adyam

Supervision: Krishnamurthy Jyothinagaram, Venimadhav Adyam

Disclosures

Acknowledgements

References

1. Singh RP, Tomy CV: Observation of magnetization reversal and negative magnetization in Sr_2YbRuO_6. Journal of Physics: Condensed Matter. 2008, 20:235209. 10.1088/0953-8984/20/23/235209
2. Banerjee A, Sannigrahi J, Giri S, Manjumdar S: Magnetization reversal and inverse exchange bias phenomenon in the ferrimagnetic polycrystalline compound Er_2CoMnO_6. Physical Review B. 2018, 98:104414. 10.1103/PhysRevB.98.104414
3. Ohkoshi S, Abe Y, Fujishima A, Hashimoto K: Design and preperation of a novel magnet exhibiting two compensation temperatures based on molecular field theory. Physical Review Letters. 1999, 82:1285. 10.1103/PhysRevLett.82.1285
4. Neel L: Magnetic properties of ferrites: ferrimagnetism and antiferromagnetism. Physical Chemical & Earth Sciences. 1984, 31:18.
5. Manna PK, Yusuf SM, Shukla R, Tyagi AK: Pole-reversal of magnetization in core-shell type $La_{1-x}Ce_xCrO_3$ (x = 0.8-1.0) nanoparticles. Journal of Physics: Conference Series. 2010, 200:072063. 10.1088/1742-6596/200/7/072063
6. Pauthenet R: Spontaneous magnetization of some garnet ferrites and the aluminum substituted garnet ferrites. Journal of Applied Physics. 1958, 29:253-55. 10.1063/1.1723094
7. Mayo J, Sui Y, Zhang X, et al.: Temperature- and magnetic-field-induced magnetization reversal in perovskite $YFe_{0.5}Cr_{0.5}O_3$. Applied Physics Letters. 2011, 98:192510. 10.1063/1.3590714
8. Ren Y, Palstra TTM, Khomskii DI, Pellegrin E, Nugroho A A, Menovsky AA, Sawatzky GA: Temperature-induced magnetization reversal in a YVO_3 single crystal. Nature. 1998, 396:441-44. 10.1038/24802
9. Sharma N, Srivastava BK, Krishnamurthy A, Nigam AK: Magnetic behaviour of the orthochromite $La_{0.5}Gd_{0.5}CrO_3$. Solid State Sciences. 2010, 12:1464-68. 10.1016/j.solidstatesciences.2010.06.007
10. Shukla R, Manjanna J, Bera AK, Yusuf SM, Tyagi AK: $La_{1-x}Ce_xCrO_3$ (0.0≤x≤1.0): a new series of solid solutions with tunable magnetic and optical properties. Inorganic Chemistry. 2009, 48:11691-96. 10.1021/ic901735d
11. Yusuf SM, Kumar A, Yakhmi JV: Temperature- and magnetic-field-controlled magnetic pole reversal in a molecular magnetic compound. Applied Physics Letters. 2009, 95:182506. 10.1063/1.3259652
12. Kumar A, Yusuf SM, Keller L, Yakhmi JV: Microscopic understanding of negative magnetization in Cu, Mn, and Fe based prussian blue analogues. Physical Review Letters. 2008, 101:207206. 10.1103/PhysRevLett.101.207206
13. Yoshii K: Magnetic properties of perovskite $GdCrO_3$. Journal of Solid State Chemistry. 2001, 159:204-8. 10.1006/jssc.2000.9152
14. Mahajan AV, Johnsto DC, Torgeson DR, Borsa F: Magnetic properties of $LaVO_3$. Physical Review B. 1992, 46:10966. 10.1103/PhysRevB.46.10966
15. Su Y, Zhang J, Feng Z, et al.: Magnetization reversal and Yb^{3+}/Cr^{3+} spin ordering at low temperature for perovskite $YbCrO_3$ chromites. Journal of Applied Physics. 2010, 108:013905. 10.1063/1.3457905
16. Yoshii K, Ikeda N, Shimojo Y, Ishii Y: Absence of a polar phase in perovskite chromite $RCrO_3$ (R=La and Pr). Materials Chemistry and Physics. 2017, 190:96-101. 10.1016/j.matchemphys.2016.12.074
17. Yoshii K: Spin rotation, glassy state, and magnetization switching in $RCrO_3$ (R = $La_{1-x}Pr_x$, Gd, and Tm): reinvestigation of magnetization reversal. Journal of Applied Physics. 2019, 126:123904. 10.1063/1.5116205
18. Coutinho PV, Moreno NO, Ochoa EA, Maia da Costa MEH, Barrozo P: Magnetization reversal in orthorhombic Sr-doped $LaFe_{0.5}Cr_{0.5}O_{3-\delta}$. Journal of Physics: Condensed Matter. 2018, 30:235804. 10.1088/1361-648x/aac06d
19. Zhang HG, Xie L, Liu XC, Xiong MX, Cao LL, Li YT: The reversal of the spontaneous exchange bias effect and zero-field-cooling magnetization in $La_{1.5}Sr_{0.5}Co_{1-x}Fe_xMnO_6$: the effect of Fe doping. Physical Chemistry Chemical Physics. 2017, 19:25186-96. 10.1039/c7cp04773h
20. Ruan MY, Li TY, Wang L, Luo QC: Magnetization sign reversal, spin-glass-like state and Griffiths-like phase driven by B-site disorder in double perovskite Gd_2CrMnO_6. Journal of Alloys and Compounds. 2023, 940:168787. 10.1016/j.jallcom.2023.168787

21. Patra KP, Ravi S: Sign reversal of both spontaneous and conventional exchange bias in nanoparticles of Y2FeCrO6 double perovskite. Journal of Applied Physics. 2022, 132:213903. 10.1063/5.0120669

22. Giri SK, Sahoo RC, Dasgupta P, Poddar A, Nath TK: Giant zero field cooled spontaneous exchange bias effect in phase separated La1.5Sr0.5CoMnO6. Applied Physics Letters. 2013, 103:252410. 10.1063/1.4855135

23. Krishnamurthy J, Chandrasekhar KD, Wu HC, Yang HD, Lin JY, Venimadhav A: Giant spontaneous exchange bias effect in Sm1.5Ca0.5CoMnO6 perovskite. Journal of Physics D: Applied Physics. 2016, 49:165002. 10.1088/0022-3727/49/16/165002

24. Patra KP, Ravi S: Antisite disorder driven spontaneous exchange bias effect in La2-xSrxCoMnO6 (0 ≤ x ≤ 1). Journal of Physics: Condensed Matter. 2016, 28:086003. 10.1088/0953-8984/28/8/086003

25. Azad AK, Mellergard A, Eriksson SG, et al.: Structural and magnetic properties of LaFe0.5Cr0.5O3 studied by neutron diffraction, electron diffraction and magnetometry. Materials Research Bulletin. 2005, 40:1633-44. 10.1016/j.materresbull.2005.07.007

26. Vijayanandhini K, Simon C, Pralong V, et al.: Zero magnetization in a disordered (La1-x/2Bix/2)(Fe0.5Cr0.5)O3 uncompensated weak ferromagnet. Journal of Physics: Condensed Matter. 2009, 21:486002. 10.1088/0953-8984/21/48/486002

27. Krishnamurthy J, Venimadhav A: Magnetization reversal phenomena and bipolar switching in La1.9Bi0.1FeCrO6. Physica B: Condensed Matter. 2014, 448:162-66. 10.1016/j.physb.2014.04.020

28. Roisnel T, Rodriguez-Carvanjal J: WinPLOTR: a windows tool for powder diffraction pattern analysis. Materials Science Forum. 2001, 378-381:118-23. 10.4028/www.scientific.net/msf.378-381.118

29. Momma K, Izumi F: VESTA 3 for three-dimensional visualization of crystal, volumetric and morphology data. Journal of Applied Crystallography. 2011, 44:1272-76. 10.1107/S0021889811038970

30. Yi K, Wu Z, Tang Q, Gu J, Ding J, Chen L, Zhu X: Microstructural characterization and magnetic, dielectric, and transport properties of hydrothermal La2FeCrO6 double perovskites. Nanomaterials. 2023, 13:3132. 10.3390/nano13243132

31. Tamine M, Nogues M, Dormann JL, Greneche JM: Magnetic clustering phenomena in a crystalline mixed ferric flouride Fe0.67Cr0.33F3. Journal of Magnetism and Magnetic Materials. 1995, 144:1765-66.

32. Yoshii K: Magnetization reversal in TmCrO3. Materials Research Bulletin. 2012, 47:3243-48. 10.1016/j.materresbull.2012.08.005

33. Zubov EE, Markovich V, Fita I, Wisniewski A, Puzniak R: Magnetic order in ErFeO 3 single crystals studied by mean-field theory. Physical Review B. 2019, 99:184419. 10.1103/PhysRevB.99.184419

34. Mahana S, Manju U, Topwal D: Complex magnetic behavior in GdCrO3. AIP Conference Proceedings. 2017, 1832:130046. 10.1063/1.4980766

35. Kumar S, Coondoo I, Vasundhara M, Patra AK, Kholkin AL, Panwar N: Magnetization reversal behavior and magnetocaloric effect in SmCr0.85Mn0.15O3 chromites. Journal of Applied Physics. 2017, 121:043907. 10.1063/1.4974737

36. Badapanda T, Senthil V, Rana DK, Panigrahi S, Anwar S: Relaxor ferroelectric behavior of "A" site deficient Bismuth doped Barium Titanate ceramic. Journal of Electroceramics. 2012, 29:117-24. 10.1007/s10832-012-9754-z

37. Biswas S, Pal S: Negative magnetization in perovskite RTO3 (R = rare-earth, T = Cr/Mn). Reviews on Advanced Materials Science. 2018, 53:206-17. 10.1515/rams-2018-0014

38. Patra KP, Ravi S: Negative magnetization and exchange bias behavior in nanocrystalline Ho2CoMn1−xNixO6 (x=0-0.4) double perovskite. Journal of Alloys and Compounds. 2022, 921:166090. 10.1016/j.jallcom.2022.166090

39. Aswathi K, Pezhumkattil Palakkal J, Revathy R, Varma MR: Sign reversal of magnetization in Sm2CrMnO6 perovskites. Journal of Magnetism and Magnetic Materials. 2019, 483:89-94. 10.1016/j.jmmm.2019.03.094